



Numerical Modelling of Harbor Agitation

Liman Çalkantılarının Sayısal Modellemesi

Olca Egriboyun^{1*}, Lale Balas¹

¹ Sea and Aquatic Sciences Application and Research Center, Engineering Faculty, Gazi University, 06570, Ankara TURKEY

Başvuru/Received: 25/01/2023 Kabul/Accepted: 29/02/2024. Çevrimiçi Basım/Published Online: 30/06./2024.
Son Versiyon/Final Version: 30/06/2024

Abstract

Two numerical models developed based on an equation of mild slope have been compared to analyze the ability of diffraction from breakwaters and reflection from coastal structures. The parabolic wave model REF/DIF1 and the elliptic wave model RIDE are used as the modeling tools. Both numerical models are applied to Darıca Fishery Port located at the Eastern Black Sea of Turkey. Different reflective structures have been used, such as quay walls, rock armor breakwater, and slipways in the port. It has been concluded that the REF/DIF-1 model can not simulate wave diffraction properly due to the parabolic approximation. However, the RIDE model can successfully handle strong diffraction and reflection from reflective structures.

Key Words

"Mild Slope Equation, REF/DIF1 model, RIDE model, wave diffraction, reflection"

Öz

Yumuşak eğim denklemine dayalı olarak geliştirilen iki farklı sayısal model, dalgakıran etrafındaki kırınım ve kıyı yapılarından yansıma kabiliyetini benzeştirmek için karşılaştırmalı olarak incelenmiştir. Modelleme araçları olarak parabolik dalga modeli REF/DIF1 ve eliptik dalga modeli RIDE kullanılmıştır. Her iki sayısal model de Doğu Karadeniz'de bulunan Darıca Balıkçı Limanı'na uygulanmıştır. Limanda rıhtım duvarları, taş dolgu dalgakıranlar ve kızaklar gibi farklı yansıtıcı yapılar kullanılmıştır. REF/DIF-1 modelinin parabolik yaklaşım nedeniyle dalga kırınımını düzgün bir şekilde simüle edemediği sonucuna varılmıştır. Bununla birlikte, RIDE modeli, yansıtıcı yapılardan kaynaklanan güçlü kırınım ve yansımayı başarılı bir şekilde benzeştirebilmektedir.

Anahtar Kelimeler

"Yumuşak eğim eşitliği, REF/DIF1 model, RIDE modeli, dalga kırınımı, dalga yansıması"

1. Introduction

Berkhoff (1972) derived an equation on mild slopes to study wave propagation under changing bathymetry conditions. This linear and elliptical equation can handle the combined effects of diffraction, refraction, and shoaling. A mild slope equation for velocity potential can be written as Eq (1).

$$\frac{\partial}{\partial x} \left(C C_g \frac{\partial \phi}{\partial x} \right) + \frac{\partial}{\partial y} \left(C C_g \frac{\partial \phi}{\partial y} \right) + \frac{\sigma^2 C_g}{C} \phi = 0 \quad (1)$$

Where σ : frequency, ϕ : potential function of velocity, C_g : group velocity, C : wave speed.

Also, the equation assumes that the bottom slope is mild. This assumption means the bathymetry variation per wavelength is slight, and the bottom contours are uniform. Wave transformation from deep to shallow water affects nonuniform bottom contours, wave breaking, bottom friction, regional currents, wave-induced currents, and wave-wave interaction (triad or quadruplet). Reflection and wave-structure interaction effects should be considered if any obstacle exists submerged or emerged in the wave propagation region.

The equation of mild slope was improved with additional terms to become more complex and realistic through much research. Solving this equation in elliptic form becomes challenging for large areas. This challenge has led to the development of different approaches to the solution. A parabolic approximation derived by Radder (1979) divides the wavefield into propagating and reflected components and ignores the reflected one. Because of this feature, the equation's parabolic form is unsuitable if strong diffraction or reflection effects are essential. A hyperbolic approximation derived by Copeland (1985) splits the original equation into a pair of first-order equations without ignoring reflection. For rapidly varying bottom topography, the slope and curvature of the bottom can be added to the equation (Lee et al., 1998). The bottom slope square is a negligible term in deep water but significant in intermediate and shallow water. Also, the curvature of the bottom is negligible in shallow and deep regions, but it is important in intermediate water. Energy dissipation occurs when waves arrive at shallow water because of the bottom friction and wave breaking. These terms can be included in the equation (KHELLAF and BOUHADF, 2004). Ambient current can affect the direction and height of waves, especially in the breaking region or around the coastal structures. Including energy dissipation and wave-current interaction terms in the equation, wave distribution can be obtained around jetties accurately (Chen et al., 2005). Nonlinear effects are also crucial in shallow regions. Nonlinear group celerity of waves can be considered to increase the correctness of the solution (Balas and İnan, 2009). Harbor resonance can also be modeled with a mild slope equation (Balas and Eğriboyun, 2023).

The mild slope equation is widely used in wave transformation and harbor studies in coastal engineering. For instance, CGWAVE (Panchnag and Demirbilek, 1998), ARTEMIS (Telemac Modelling System, 2012), PHAROS (Deltares, 2013), and MIKE21 EMS and MIKE21 PMS (DHI, 2011) are the most famous wave models which are developed with mild slope equations. This study uses two open-source numerical wave models based on mild slope equations. The first is the parabolic wave model REF/DIF1 (Kirby and Dalrymple 1994), and the second is the elliptic wave model RIDE (Maa et al., 2002). Two models are explained in detail and applied to Darica Fishery Port in the Eastern Black Sea of Turkey.

2. REF/DIF1 Wave Model

REF/DIF1 is a weakly nonlinear parabolic wave model developed by Kirby and Dalrymple (1994). REF/DIF1 can simulate refraction, diffraction, shoaling, wave-current interaction, energy dissipation from bottom friction, and wave breaking. Known ambient currents, which affect the wave height and wave direction of wave transformation, are input for the model and enable it to predict waves where currents may be substantial. The parabolic approximation assumes that the wave propagates primarily in one direction and disallows backward propagating waves. Since the model uses parabolic approximation, it can not correctly consider the reflection effects. With this feature, the boundary condition at the down wave end of the model area is no longer necessary. Only initial and lateral boundary conditions are required. Due to the neglect of the backward propagating waves, the model cannot be used in areas where reflection effects are essential, such as harbors. REF/DIF-1 parabolic wave model can handle larger domains with larger grid spacing than elliptical solutions. The grid resolution should generally be at least five meshes per wavelength.

Parabolic Eq (2) for wave diffraction for constant depth was developed by Mei and Tuck (1980).

$$\frac{\partial A}{\partial x} = \frac{i}{2k} \frac{\partial^2 A}{\partial y^2} \quad (2)$$

Where A: wave amplitude in complex variable form related to the water surface displacement given in Eq(3).

$$\eta = Ae^{i(kx-\sigma t)} \tag{3}$$

Yue and Mei [16] developed a nonlinear form of Eq(2) for the propagation of a third-order Stokes wave by a multiple scales approach given in Eq(4).

$$2i \frac{\partial A}{\partial x} + \frac{1}{k} \frac{\partial^2 A}{\partial y^2} - K'|A|^2 A = 0 \tag{4}$$

$$K' = k^3 \left(\frac{C}{C_g} \right) D \tag{5}$$

$$D = \frac{\cos 4kh + 8 - 2 \tanh^2 kh}{8 \sinh^4 kh} \tag{6}$$

where $i = \sqrt{-1}$, C: wave celerity, Cg: group velocity, D: nonlinear coefficient.

REF/DIF1 was developed by combining the main features of the approaches mentioned above, preserving the variable depth feature of the mild slope equation and additional terms. REF/DIF1 combines the nonlinear diffraction equation with the linear mild slope equation. REF/DIF1 has weak cubic nonlinearity (cubic because of the triple product of unknown amplitudes). This weak nonlinearity resulted from Stoke's third-order perturbation expansion and was first derived for use in a parabolic mild slope model (Kaihatu, 1997). As a result, the model equation obtained in Equation (7) and this Equation expanded with energy dissipation and current terms.

$$2ikCC_g \frac{\partial A}{\partial x} + 2k(k - k_0)(CC_g)A + i \frac{\partial(kCC_g)}{\partial x} A + \frac{\partial}{\partial y} \left(CC_g \frac{\partial A}{\partial y} \right) - k(CC_g)K'|A|^2 A = 0 \tag{7}$$

REF/DIF1 wave model discretized with Crank-Nicholson finite difference scheme. The implicit solution method provides second-order accuracy in the x and y directions. The Crank-Nicholson method consists of central and forward differences for the derivatives of second and first order. The unknowns at $i + 1$ row can be solved in terms of known values at the i 'th row. Figure 1 shows the computational molecule that outlines the scheme. Grid spacings Δx and Δy in the horizontal directions can be chosen differently.

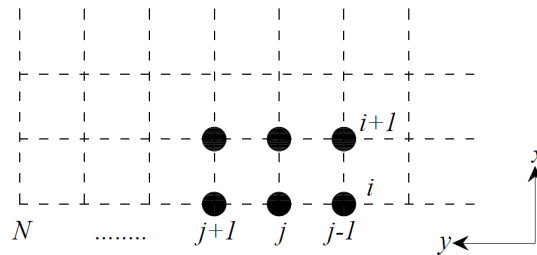


Figure 1. Grid Definition for REF/DIF1 and Crank-Nicholson Computational Molecule

Energy dissipation from bottom friction can be considered in the model in three different ways. The first one is the laminar surface and bottom boundary layer. Boundary layers develop at the water surface and the bottom due to viscosity. A significant amount of damping occurs for a contaminated surface that depends on the fluid's viscosity. Energy dissipation because of laminar surface and bottom boundary layers can be estimated depending on the kinematic viscosity. The second one is the turbulent bottom boundary layer. The Darcy-Weisbach friction in the model estimates this kind of energy dissipation. The third one is the porous sand. Wave propagation over porous sand induces a flow into the seabed, resulting in wave damping due to the Darcy flow. The model's permeability coefficient considers such energy dissipations due to sandy sea bottom.

Energy dissipation caused by the breaking of waves is based on the model of Dally et al. (1985). This dissipation mechanism assumes that once breaking has occurred, the energy flux tends toward a stable value, and the rate of loss of energy flux depends on the amount of flux over this stable value. The breaking index (wave height/water depth) is assumed to be 0.78 in the model. Wave-breaking induced

energy dissipation arises, meeting the criteria. The mechanism of dissipation due to breaking is always active in the model, whereas the user activates the dissipation mechanism due to bottom friction.

There are two main boundary conditions in the model: initial and lateral boundary conditions. The initial boundary condition defines the wave amplitude ($a=H/2$), period, and direction at the offshore grid row. The model calculates complex amplitudes along the offshore boundary using input parameters. Two options are available for the lateral boundary conditions: open or closed. The conditions for lateral boundaries must be defined to limit the computational area when no shorelines are on the left and right sides.

These are the waters surrounding the boundary of the computational waters. Waves enter and leave the model domain without reflection by the proper definition of condition for an open boundary. However, this boundary definition in the model may not allow complete transmission, i.e., some reflected waves in the domain may still exist. A closed boundary condition means a reflective boundary. The model domain must be carefully selected because waves may return to the model domain at the closed boundaries.

The lateral boundary conditions may be taken considerably at large horizontal distances to eliminate interaction with the wave scattering, especially for oblique waves. A typical model domain is shown in Figure 2. REF/DIF1 v2.5, written in Fortran programming language, is used in this study.

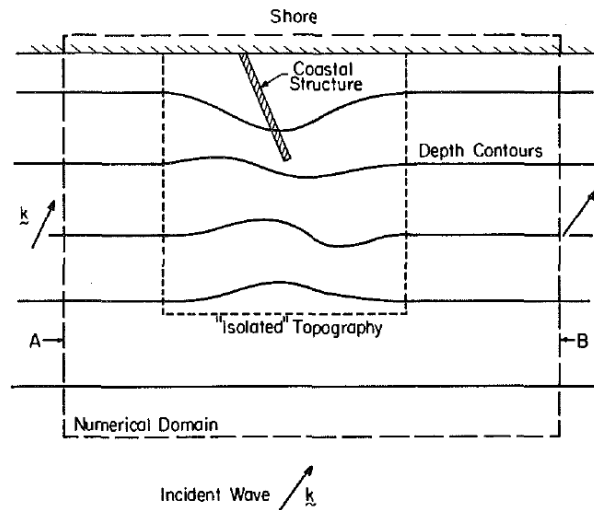


Figure 2. Recommended Numerical Model Domain (A and B are lateral boundaries)

3. RIDE Wave Model

The RIDE Wave Model is an elliptic wave model developed by Maa et al. (2002). RIDE can consider shoaling, refraction, reflection, diffraction, curvature, the slope of the bottom, and dissipation of energy due to the breaking of waves and friction at the sea bed.

The RIDE model can consider the reflection effects from the reflective structures (i.e., breakwater, quay wall, etc.) in the domain, both forward and backward propagating waves. Because of that, it is necessary to define all boundary conditions in the domain. The model does not contain nonlinear terms. The RIDE model can be used in areas with essential reflection effects, such as harbors. Compared to parabolic model solutions, the RIDE elliptic wave model can handle smaller domains with smaller grid spacings. The grid resolution should generally be at least ten meshes per wavelength.

The extended mild slope Eq(8) was used in the RIDE model (Suh et al., 1997). The curvature factor at the bottom is given in Eq(9). Eq(10) gives the factor for the bottom slope. These factors depend on the water depth and wave number (Hsu and Wen, 2001).

$$\nabla \cdot (CC_g \nabla \phi) + k^2 CC_g (1 + i f \phi) + [f_1 g \nabla^2 h + f_2 (\nabla h)^2 g k] \phi = 0 \tag{8}$$

$$f_1 = \frac{\sinh(kh) + \sinh(3kh) - 4kh \cosh(kh) + 8(kh)^2 \sinh(kh)}{8 \cosh^3(kh) [\sinh(2kh) + 2kh]} - \frac{k h \tanh(kh)}{2 \cosh^2(kh)} \tag{9}$$

$$f_2 = \frac{\operatorname{sech}^2(kh)}{6[2kh + \sinh(2kh)]^3} \{16(kh)^3 \sinh(2kh) + 8(kh)^4 + 12(kh)[1 + 2\sinh^4(kh)][kh + \sinh(2kh)] - 9\sinh^2(2kh)\cosh(2kh)\} \quad (10)$$

where, ∇h : bottom slope, ϕ : potential function for velocity in simple harmonic wave field, $\nabla^2 h$: bottom curvature, $f = f_d + f_b$: Combined energy dissipation factor. The friction factor of the bottom for non-breaking waves, f_b , is given in Eq(11), and the dissipation factor of energy for breaking waves, f_d , is given in Eq(12).

$$f_b = \frac{4C_f}{3\pi} \frac{a\omega^2}{ng\sinh^3 kh} \quad (11)$$

$$f_d = \frac{k_2}{kh} \left(1 - \frac{k_1^2}{4\gamma^2}\right) \quad (12)$$

$$n = \frac{1}{2} \left(1 + \frac{2kh}{\sinh 2kh}\right) \quad (13)$$

Where $k_1 = 0.4$ and $k_2 = 0.15$ are empirical constants, C_f : wave friction factor, a : wave amplitude, ω : angular wave frequency, and $a/h = \gamma$ is wave amplitude to the depth of water ratio.

The RIDE wave model is discretized with a five-point finite difference scheme. Gaussian elimination is applied to the solution of the banded matrix produced. In the classical Gaussian elimination method, round-off errors can cause problems regarding the convergency. The partial pivoting method is used to reduce this problem. The partial pivoting method increases the processing load and the solution's stability. Because of the small grid sizes for solving the elliptic mild slope equation, a large band matrix may develop that needs bigger computer memory (RAM). The RIDE model uses a bookkeeping procedure to replace the requirement for the large memory of a computer with a large hard disk. The band matrix splits into small matrices. Figure 3 shows the computational molecule of the scheme.

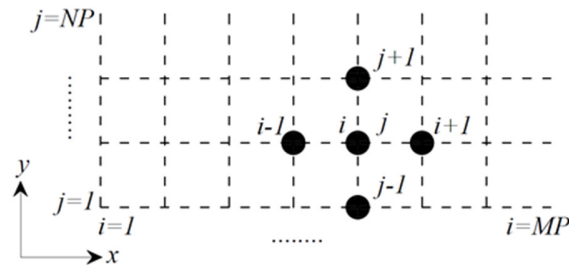


Figure 3. Grid Definition for RIDE Model and 5-Point Computational Molecule

Energy dissipation from the laminar surface and bottom boundary layer can be estimated depending on kinematic viscosity. The model considers energy dissipation because of friction at the bed in 3 ways, similar to REF/DIF1. The wave friction factor and the permeability coefficients are used respectively to consider the turbulent bottom boundary layer and the energy dissipation from the sandy sea bottom.

The breaking index (wave height/water depth) is 0.78 in the REF/DIF1 wave model. The RIDE model calculates wave parameters in the first run and stores these values in a file. Because of wave breaking, the model must be run again to calculate energy dissipation. The user can activate the dissipation mechanism due to the breaking of waves and friction at the bottom. The model has two main boundary conditions: reflection and given boundary conditions. The reflection boundary condition creates three different situations according to the value of the reflection coefficient. R being the coefficient of reflection, the reflective grids are defined with Eq(14) and Eq(15) for boundaries perpendicular to the x and y axis, respectively. The absorption coefficient (α) is obtained by $\alpha = (1-R)/(1+R)$. $R=1$ and $\alpha=0$ mean full reflection. $R=0$ and $\alpha=1$ mean no reflection. If $0 < R < 1$, partial reflection occurs, vital for realistic harbor studies.

$$\frac{\partial \phi}{\partial x} = \pm i\alpha k \left(\phi + \frac{1}{2k^2} \frac{\partial^2 \phi}{\partial y^2} \right) \quad (14)$$

A given boundary condition defines the wave height, period, and direction at the offshore grid in a row. Eq(16) and Eq (17) are used at a given boundary with no reflection. The velocity potential is calculated by Eq(18) with the given wave parameters.

$$\frac{\partial \phi}{\partial x} = \pm ik \left(\phi + \frac{1}{2k^2} \frac{\partial^2 \phi}{\partial y^2} \right) + 2ik\phi^g \tag{15}$$

$$\frac{\partial \phi}{\partial y} = \pm ik \left(\phi + \frac{1}{2k^2} \frac{\partial^2 \phi}{\partial x^2} \right) + 2ik\phi^g \tag{16}$$

$$\phi^g = Ae^{is} = \frac{igTH}{4\pi} e^{is} \tag{17}$$

The boundary definition is shown in Figure 4. The right and left boundaries are located on the right and left sides of the computational domain, and the bottom and the top boundaries are defined on the domain's downside and the upper side.

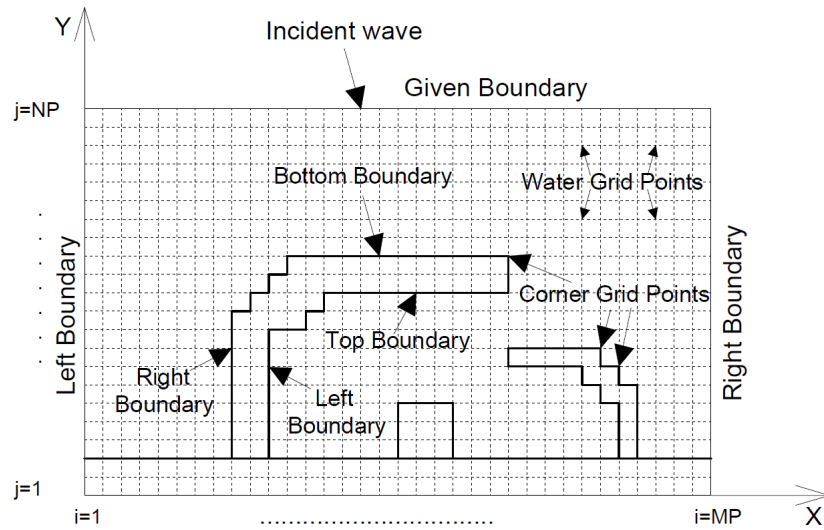


Figure 4. Boundary Definitions for the RIDE Model

Boundary definition rules are taken from the model computer code and summarized in Table 1. A demonstration is shown in Figure 5 according to Figure 4. After the boundary definitions are done, the absorption coefficients are defined depending on the reflection coefficients in the mesh points. The RIDE wave model uses the Fortran programming language as well.

Table 1. Boundary Definition Rules in the RIDE Model

Value	Definition	Value	Definition
0	Water grid points	5	Corner at bottom left
1	Top boundary	6	The corner at the top left
2	Bottom boundary	7	Corner at bottom right
3	Left boundary	8	Corner at top right
4	Right boundary	g	Given boundary
e	Land grid points	o	left bottom corner, if a wave comes from the bottom boundary
p	left bottom corner, if the wave comes from the left boundary	q	left top corner, if the wave comes from the left boundary
r	left top corner, if the wave comes from the top boundary	s	right top corner, if the wave comes from the top boundary
t	right top corner, if the wave comes from the right boundary	u	right bottom corner, if the wave comes from the right boundary
v	right bottom corner, if the wave comes from the bottom boundary		

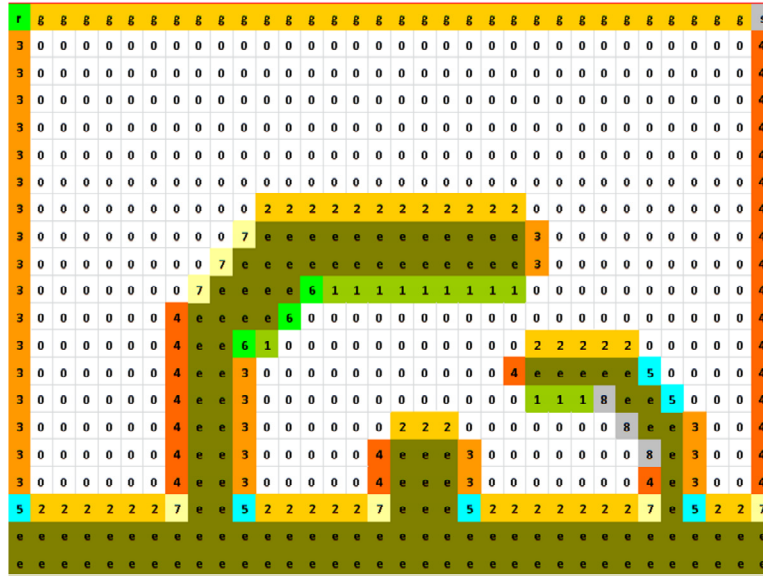


Figure 5. Boundary Definition with Boundary Values in RIDE Model

4. Case study at Darıca Fishery Port

Both models have been applied to the Darıca Fishery Port (Figure 6) as the case study area in the Eastern Black Sea. The model domain (Figure 7) has 0.9 km and 1.9 km in the x (wave propagation direction) and y directions, respectively. The area of interest is a fishery port. Thus, it is located in the middle of the domain. The geographic coordinates of the area are 41.052071°N and 39.539033°E. The maximum water depth is -35 m. The parameters of the case study are shown in Table 2. Waves are approaching from NE, perpendicular to the y-direction. Incident waves are coming perpendicular to the model domain.

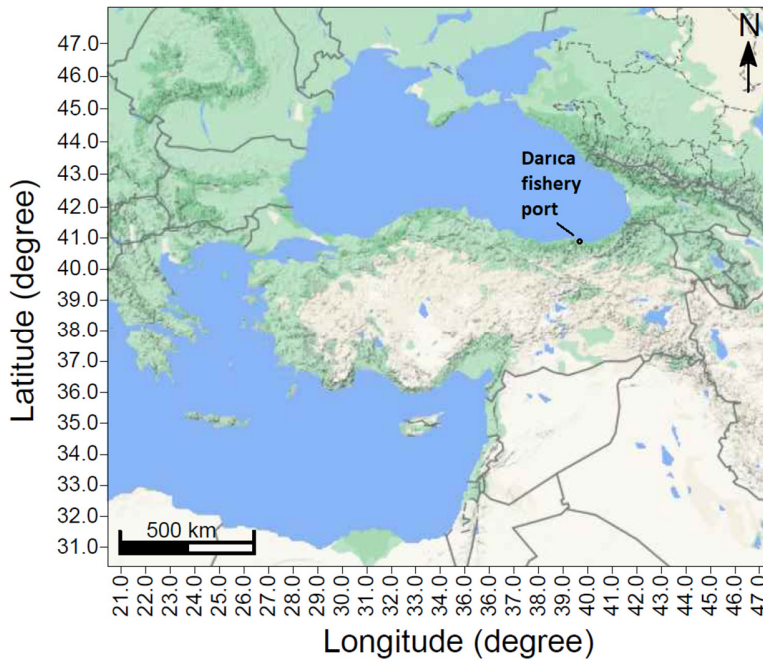


Figure 6. Geographical Location of Darıca Fishery Port

Table 2. Parameters of the Case Study

Wave Model	H (m)	T (s)	Incident wave angle (°)	Grid Spacing (m)	Grid Dimension (x direction)	Grid Dimension (y direction)	Lateral Boundary Conditions
RED/DIF1	2.0	6.0	0	12	75	160	Reflective
RIDE	2.0	6.0	0	6	150	320	Reflective

Green areas of the port are quay walls, the red area is a slipway, and other parts of the port are rubble mound breakwater with quarry stone armor layer (Figure 8). According to reflective areas, absorption and reflection coefficients are shown in Table 3 for the RIDE wave model. Absorption coefficients are calculated according to the reflection coefficients shown in Table 4 (Thompson et al., 1996). The boundary definition of the port for the RIDE model is shown in Figure 9. Energy dissipation from wave breaking and energy dissipation from bottom friction with a turbulent bottom boundary layer are considered in both models.

Table 3. Absorption and Reflection Coefficients in the RIDE Model

Reflective Area	Reflection Coefficient (R)	Absorption Coefficient (α)
Quay Wall	0.90	0.05
Slipway	0.10	0.81
Breakwater	0.40	0.43
Land	0.00	1.00

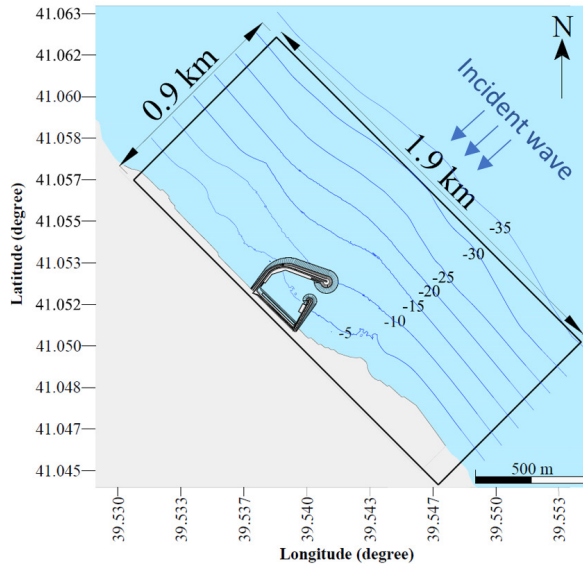


Figure 7. Domain of the Case Study

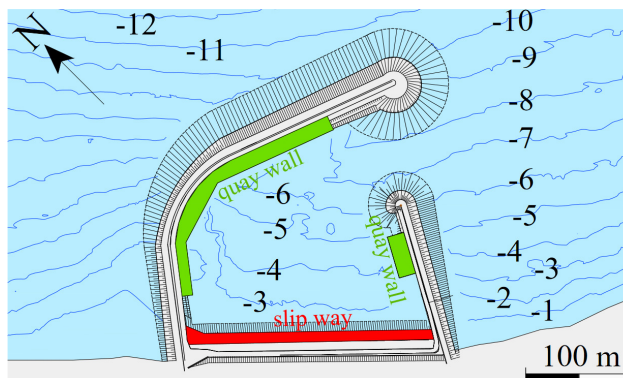


Figure 8. Reflective Areas of the Fishery Port

Table 4. The Coefficient of Reflection Values for Short Waves [21]

Vertical wall	Reflection Coefficient (R)
CAW (Crown Above Water)	1.0-0.7
Submerged Crown	0.7-0.5
Tick Rubble Toe Protection	0.6-0.4
Crown Above Water	0.6-0.4
Vertical Energy-Dissipator	0.8-0.3
Impermeable Smooth Slope	
CAW sloped 1:1.5 to 1:2.5	0.9-0.5
Submerged Crown sloped 1:1.5	0.5-0.3
Rough Slope	
1:1.5 to 1:3 sloped Rubble	0.6-0.3
Rubble less than 1:3 slope	0.25-0.1
Concrete Blocks Energy-Diss.	0.5-0.3
Permeable Breakwater, Rough,	
1:1.5 sloped Rubble	0.6-0.2
1:2.6 sloped Rubble	0.4-0.1
1:1.5 to 1:3 sloped Dolos	0.4-0.1
Natural Beach	0.2-0.05

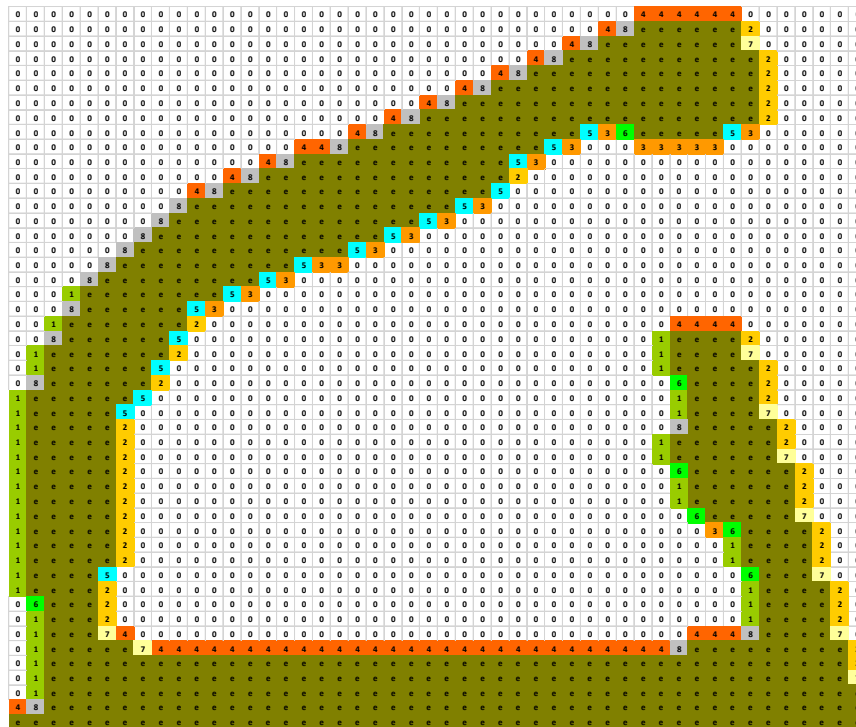


Figure 9. Boundary Definition of the Port for RIDE Model

As a result of the modeling, it is seen that the RIDE model (Figure 10) and REF/DIF1 model (Figure 11) calculate different wave distributions, especially within the port. Since the RIDE model can consider the reflection effects, the wave height increases on the seaside of the breakwater, which does not occur in the results of the REF/DIF-1 wave model. Especially in front of the quay walls, wave heights increase in the RIDE model, and wave distribution is more homogeneous than REF/DIF1. Waves entering the port are concentrated towards a particular region in the REF/DIF1 model. Wave height distribution in port is zoomed in Figure 12 for the RIDE and REF/DIF1 model results.

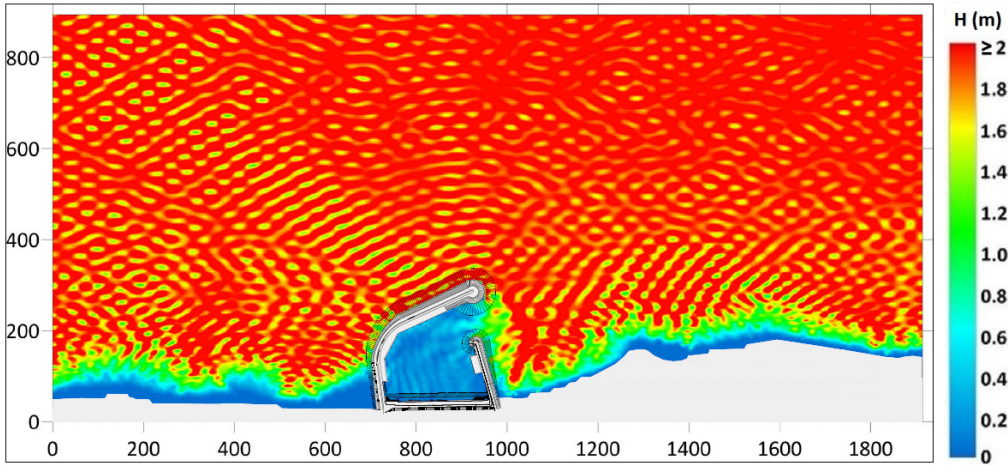


Figure 10. Computation Result of RIDE Model (Full Domain)

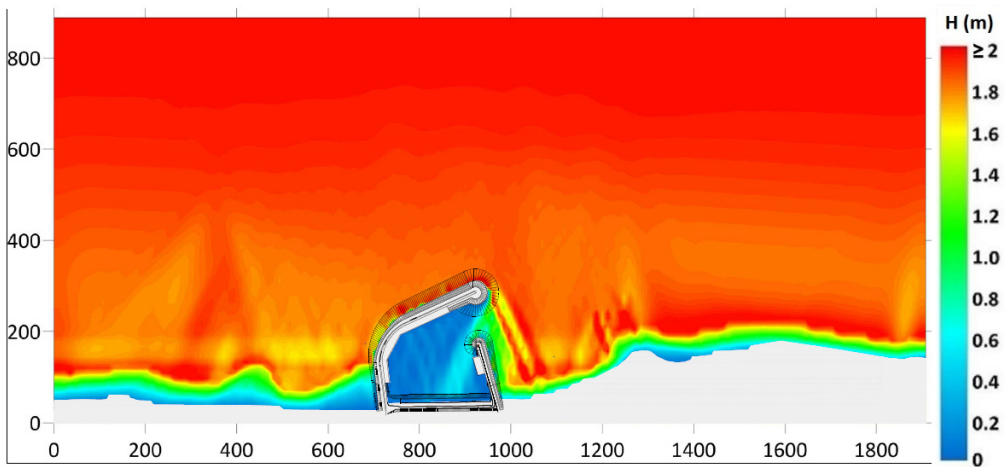
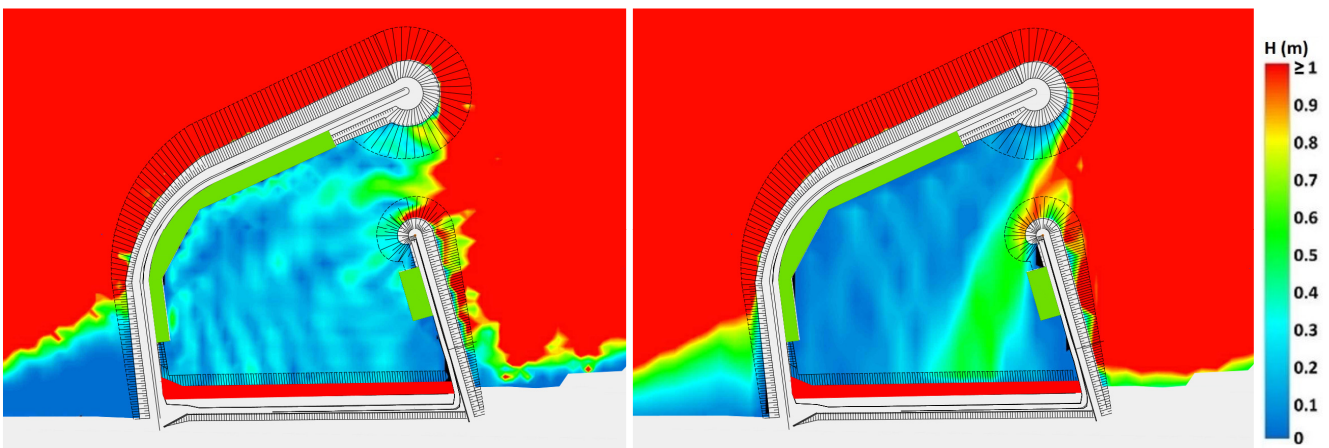


Figure 11. Computation Result of REF/DIF1 Model (Full Domain)



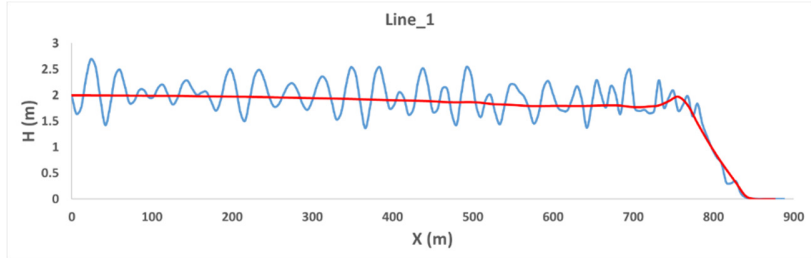
(a) RIDE Model

(b) REF/DIF1 Model

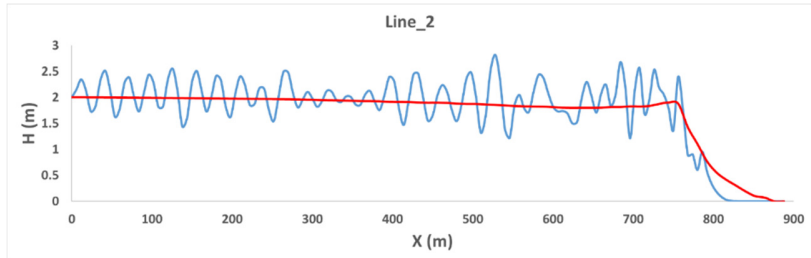
Figure 12. Computation Results in Fishery Port a) RIDE Model, b) REF/DIF1 Model

The comparison of the results of the models outside the port is presented graphically in Figure 14, along the lines in Figure 13. Line 1 is located 500 m west of the port; line 2 is located at the western boundary of the port; line 3 is located in the middle of the port; line 4 is located at the eastern boundary of the port; and line 5 is located 500 m east of the port. The wave parameter at the given boundary provides the deep water condition. Parallel to the decrease in depth during wave propagation, a decrease in wave height should also occur due to the shoaling effect. The main breakwater of the port is positioned at a depth of $d = -10$ m. Since the wave propagation is perpendicular to the bottom contours, when the refraction coefficient is taken as $K_r = 1.00$ and the shoaling coefficient is taken as K_s

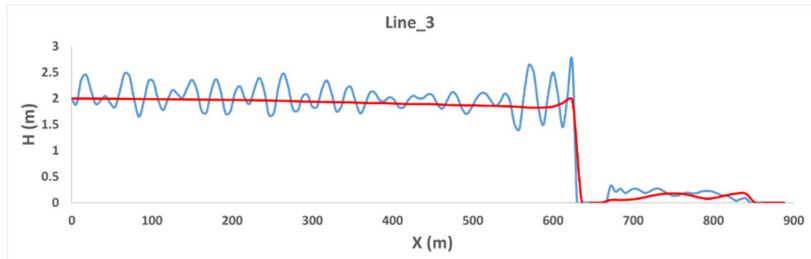
= 0.914, the wave height at $d = -10$ m depth is calculated as $H = 1.828$ m according to the linear wave theory ($H = H_0 K_r K_s$). This value was determined with the REF/DIF1 wave model as $H = 1.8335$ m. Figure 14 shows that the wave height results of the REF/DIF1 wave model decrease towards the coast in the absence of reflection because of shoaling. However, when the calculation includes the reflection effects, the shoaling effect cannot be clearly visible in the model results. While a straight line forms in the REF/DIF1 model results, an undulation occurs in the wave height in the RIDE model results due to the reflection effect. In the RIDE wave model, an increase in wave height is observed as the port approaches. This phenomenon is caused by waves reflected from the main breakwater. Additionally, the reflected waves cause higher wave heights on lines 1, 2, and 3 than on the other lines due to the arrangement of the breakwater.



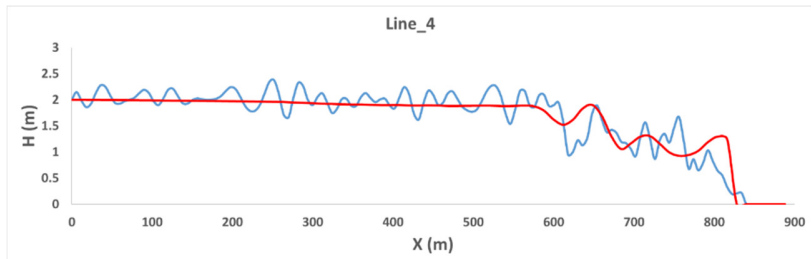
a) Comparison of Two Models at Line 1 (500 m west of the port)



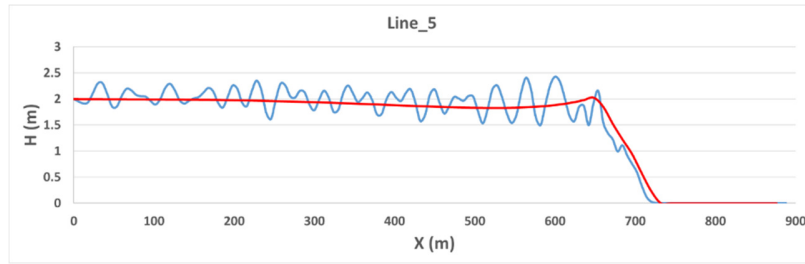
b) Comparison of Two Models at Line 2 (western boundary of the port)



c) Comparison of Two Models at Line 3 (middle of the port)



d) Comparison of Two Models at Line 4 (the eastern boundary of the port)



e) Comparison of Two Models at Line 5 (500 m east of the port)

Figure 13. Comparison Lines Outside the Port (Blue lines denote the RIDE model, red lines denote the REF/DIF1 model)

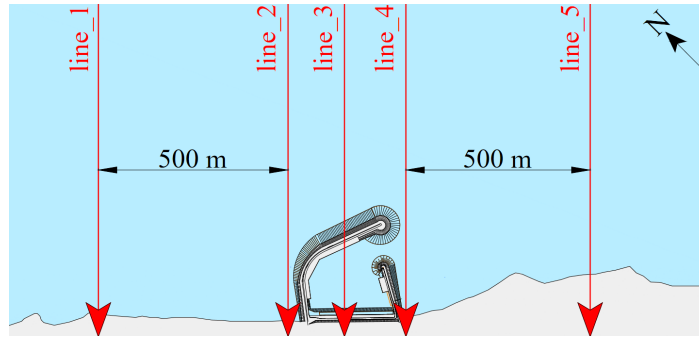


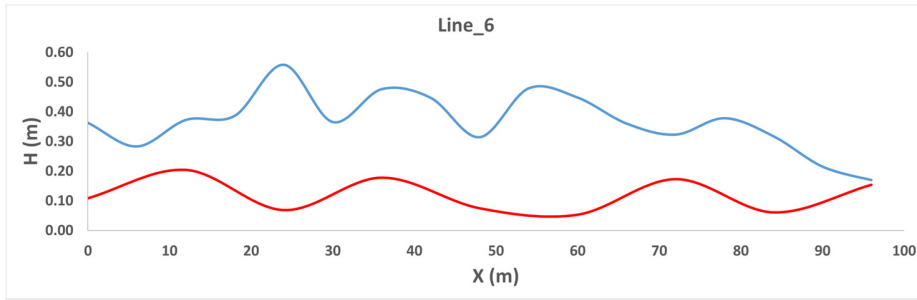
Figure 14. Comparison Lines Outside the Port (arrows show the direction of the lines. The straight end symbolizes the beginning, while the arrowed end represents the end)

The comparison of the results of the models inside the port is presented graphically in Figure 15, along the lines in Figure 16. Line 6, line 7, and line 9 are located in front of the quay walls. Line 8 is located in front of the slipway. The major difference between the two models is considering the reflection effect. While the reflection effect is considered in the RIDE wave model, it is not in the REF/DIF1 wave model. Lines 6 and 7 show wave heights at the quay wall located on the main breakwater. These quays are positioned opposite the harbor entrance. So, waves diffracted from the main breakwater head directly reach this location. At the same time, the average wave height at line 6, line 7, and line 9 in the RED/DIF1 model is $H=0.12$ m, $H=0.07$ m, and $H=0.48$ m, in the RIDE model, $H=0.37$ m, $H=0.35$ m, and $H=0.27$ m, respectively. The average wave height at line 8 in the RED/DIF1 model is $H=0.21$ m, and in the RIDE model, $H=0.20$ m. Wave heights at lines 6 and 7 in the REF/DIF1 model are much lower than in the RIDE model because of weak diffraction and the absence of reflection (Figure 15a, Figure 15b). Due to weak diffraction, wave energy concentrated to a certain location in the port at between 100-160 m on line 8 (Figure 15), so REF/DIF1 overestimated wave heights at this location. Although the average wave height of the two models in line 9 is equal, REF/DIF1 calculated higher wave heights at the beginning of the quay and a lower wave height at the end of the quay. These results show that wave agitation in a port can be simulated with the RIDE wave model.

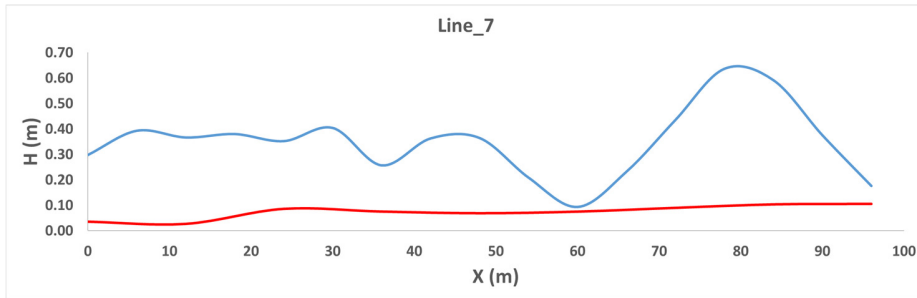
According to linear wave theory, wave height (non-diffracted) at the main breakwater head is $H=1.82$ m. If pure wave diffraction is considered with a flat bottom ($d=-10$ m) according to the diffraction diagram (Figure 17), average diffraction coefficients are obtained as $K'=0.15$ at line 6, $K'=0.15$ at line 7, and $K'=0.26$ at line 8, and $K'=0.40$ at line 9. According to diffraction coefficients, mean wave heights are expected $H=1.82 \times 0.15 = 0.27$ m at line 6, $H=1.82 \times 0.15 = 0.27$ m at line 7, $H=1.82 \times 0.26 = 0.47$ m at line 8, and $H=1.82 \times 0.40 = 0.73$ m at line 9. The waves rotate by about 60° during diffraction while entering the basin. Meanwhile, the depth at the port entrance decreases from $d=-10$ m to $d=-7$ m. Because of diffraction, refraction occurs. So, the refraction coefficient is obtained at the harbor entrance as $K_r=0.707$. Additionally, as the depths within the port decreased, the shoaling coefficient was obtained as $K_s=0.945$ for line 6, $K_s=1.045$ for line 7 and line 8, and $K_s=0.996$ for line 9. According to linear wave theory, expected wave heights $H=1.82 \times 0.15 \times 0.707 \times 0.945 = 0.18$ m at line 6, $H=1.82 \times 0.15 \times 0.707 \times 1.045 = 0.20$ m at line 7, $H=1.82 \times 0.25 \times 0.707 \times 1.045 = 0.34$ m at line 8, and $H=1.82 \times 0.40 \times 0.707 \times 0.996 = 0.51$ m at line 9 (Table 5). Wave heights inside the port, calculated according to linear wave theory, decrease as in the models.

Table 5. Comparison of the Wave Heights at Lines

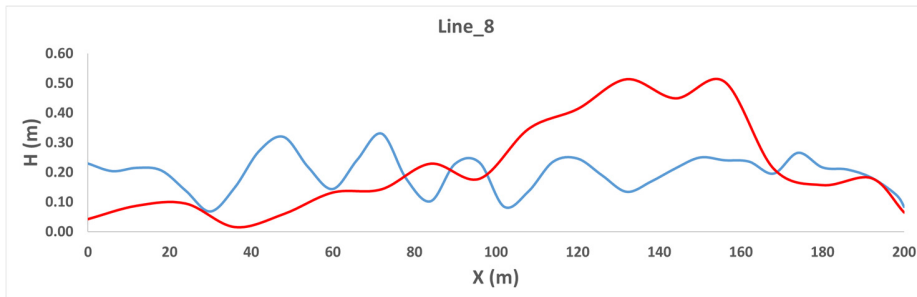
	Linear Wave Theory	REF/DIF1	RIDE		Line 6	Line 7	Line 8	Line 9
Line 6	0.18	0.12	0.37	K'	0.15	0.15	0.25	0.40
Line 7	0.20	0.07	0.35	K _r	0.707	0.707	0.707	0.707
Line 8	0.34	0.48	0.27	K _s	0.945	1.045	1.045	0.996
Line 9	0.51	0.21	0.20					



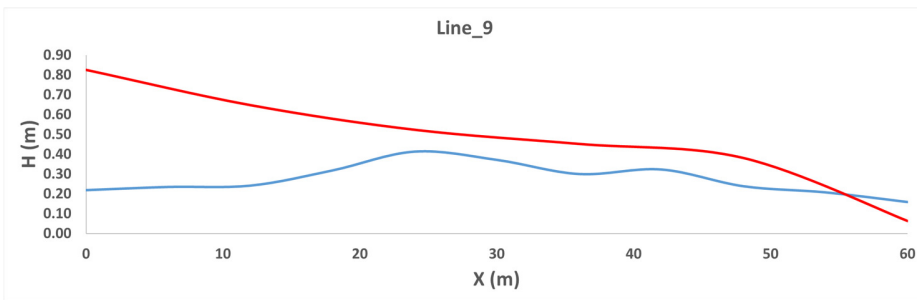
a) Comparison of Two Models at Line 6 (In front of the quay wall)



b) Comparison of Two Models at Line 7 (In front of the quay wall)



c) Comparison of Two Models at Line 8 (In front of the slipway)



d) Comparison of Two Models at Line 8 (In front of the quay wall)

Figure 15. Comparison Lines Inside the Port (Blue lines denote the RIDE model, red lines denote the REF/DIF1 model)

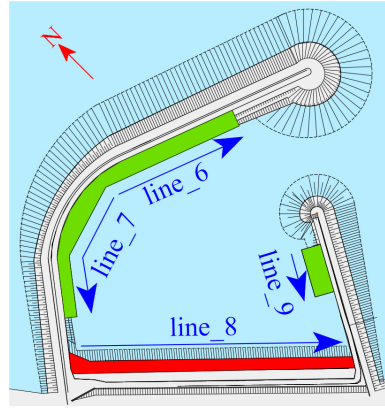


Figure 16. Comparison Lines Inside the Port (arrows show the direction of the lines. The straight end symbolizes the beginning, while the arrowed end represents the end)

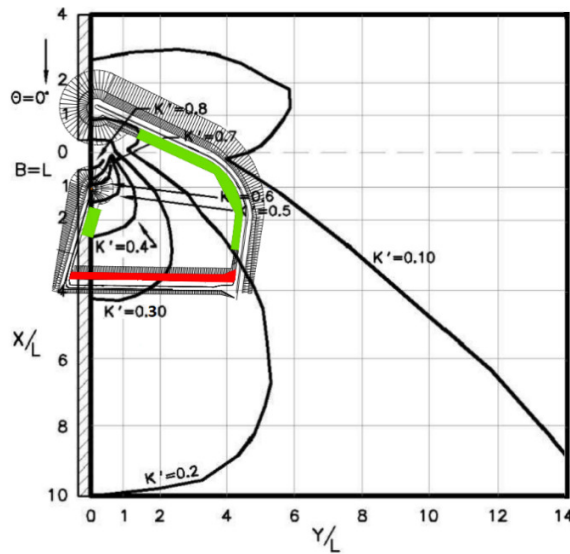


Figure 17. Wave Diffraction Diagram (Incoming wave angle, $\Theta=0^\circ$) (CEM, 2002)

5. Conclusions

REF/DIF-1 parabolic wave model and RIDE elliptic wave model are examined in detail. Both models are applied to Darıca Fishery Port, located at the Eastern Black Sea coastline, as the case study area in Turkey. The RIDE wave model predictions show that strong diffraction and reflection effects can successfully be simulated. The REF/DIF1 wave model can simulate diffraction rather weakly. The wave height results from the REF/DIF1 model were lower than those from the RIDE model at the quays due to weak diffraction and the absence of reflection inside the port. Weak diffraction in REF/DIF1 caused wave energy to concentrate in a specific location within the port, resulting in overestimating wave heights at the slipway. In contrast, in the RIDE model, waves diffracted from the breakwater head are directed homogeneously throughout the entire basin and reflected from the quays.

Two models produce comparable results outside the port where there is no obstacle. The major difference between the two models lies in considering the reflection effect. The REF/DIF1 wave model demonstrates a decrease in wave height towards the coast without reflection, mainly due to shoaling. In contrast, when considering reflection effects in the RIDE model, the shoaling effect becomes less evident in the results. Unlike the straight line observed in the REF/DIF1 model, the wave height in the RIDE model exhibits undulations caused by the reflection effect. Consequently, the RIDE wave model indicates an increase in wave height as the port is approached.

The REF/DIF1 model calculates the direction of wave propagation using a parabolic approximation, which omits reflection effects. This allows the model to provide results swiftly over large areas concerning wave propagation. In contrast, the RIDE model, employing an elliptical approach, can calculate both wave propagation and reflections. Because of the approximation, the RIDE model requires a smaller grid size than the REF/DIF1 model and may result in longer computation times, potentially extending to several days for the same-sized work area.

As a result, the REF/DIF1 model is more suitable for simulating wave transformations without emerged structures, whereas the RIDE model excels in harbor studies due to its superior simulation of diffraction and reflection effects.

References

- Balas, L. & İnan, A. (2009). Numerical Modeling of Extended Mild Slope Equation with Modified Mac Cormack Method. *Wseas Transactions On Fluid Mechanics*, 4, 14-23.
- Berkhoff, J.C.W. (1972). Computation of combined refraction–diffraction. In: *Proceedings of the 13th International Conference on Coastal Engineering*, ASCE, 1, 471–490.
- Chen, W., Panchang, V. & Demirebilek, Z. (2005). On the modeling of wave–current interaction using the elliptic mild-slope wave equation. *Ocean Engineering*, 32, 2135-2165.
- Copeland, G.J.M. (1985). A practical alternative to the mild-slope wave equation. *Coastal Engineering*, 9, 125-149.
- Dally, W.R., Dean, R.G. & Dalrymple R.A. (1985). Wave height variations across beach. *Journal of Geophysical Research*, 90, 11,917-11,927.
- Danish Hydraulic Institute, (2011). MIKE 21 elliptic mild-slope wave module. Holsholm- Denmark. Danish Hydraulic Institute.
- Deltares, 2013. PHAROS - user & technical manual - version 9.11.19731 Deltares, Delft-Netherlands
- Hsu T.-W. & Wen C.-C. (2001). A parabolic equation extended to account for rapidly varying topography, *Ocean Engineering*, 28: 1479–1498.
- Kaihatu, J.M. (1997). Review and Verification of Numerical Wave Models for Near Coastal Areas - Part 1: Review of Mild Slope Equation, Relevant Approximations, and Technical Details of Numerical Wave Models. Naval Research Laboratory Oceanography Division, Arlington ABD, 1-27.
- Khellaf, M.C. & Bouhadeb, M. (2004). Modified mild slope equation and open boundary conditions. *Ocean Engineering*, 31, 1713–1723.
- Kirby, J. T. & Dalrymple, R. A. (1994). Combined Refraction/Diffraction Model REF/DIF 1 Version 2.5 Documentation and User's Manual. Center for Applied Coastal Research Department of Civil Engineering University of Delaware, Newark, CACR Report No. 94-22, 1-172.
- Lee, C., Park, W. S., Cho, Y. S. & Suh, K. D. (1998). Hyperbolic mild-slope equations extended to account for rapidly varying topography. *Coastal Engineering*, 34, 243-257.
- Maa J.P.-Y., Hsu T.-W. and Lee D.-Y. 2002. "The RIDE model: an enhanced computer program for wave transformation", *Ocean Engineering*, 29, 1441–1458.
- Mei, C.C. & Tuck E.O. (1980). Forward scattering by thin bodies. *SIAM Journal on Applied Mathematics*, 39, 178–191.
- Panchang, V. & Demirebilek Z. (1998). CGWAVE: A Coastal Surface Water Wave Model of the Mild Slope Equation. US Army Corps of Engineers, Washington.
- Radder, A.C. (1979). On the parabolic equation method for water-wave propagation. *Journal of Fluid Mechanics*, 95, 159-176.
- Suh K.D., Lee C. & Park W.S. (1997). Time-dependent equations for wave propagation on rapidly varying topography, *Coastal Engineering*, 32: 91-117
- Telemac Modelling System (2012). Theoretical note and user manual version 6.2 Artemis software wave agitation, France. 1-138
- Thompson, E.F., Chen, H.S. & Hadley, L.L. (1996). "Validation Of Numerical Model For Wind Waves And Swell In Harbors". *Journal of Waterway, Port, Coastal, And Ocean Engineering*, 122, 245-257.
- Yue, D.K.P. & Mei, C.C. (1980). Forward Diffraction Of Stokes Waves By A Thin Wedge. *Journal of Fluid Mechanics*, 99, 33-52.

Balas, L., Eđriboyun, O. (2023). Effect of Diffracted Waves on Harbor Resonance. *Thalassas* 39, 243–261. <https://doi.org/10.1007/s41208-022-00501-w>

U.S. Army Corps of Engineers, (2002), Coastal Engineering Manual (CEM), Engineer Manual 1110-2-1100, U.S. Army Corps of Engineers, Washington, D.C. (6 volumes).